

In silico analysis of interaction of Eugenol, cis-Isoeugenol and Methyl Eugenol with the binding site of spike protein of SARS-CoV19 virus

Neeta Azad^{1*}, Neha Sharma², Esha Arora³, Priyanshi Gupta¹, Deepanshu¹

¹Department of Chemistry, Atma Ram Sanatan Dharma College, University of Delhi, New Delhi-110021

²Department of Chemistry, Gargi College, University of Delhi, New Delhi-110049

³Department of Chemistry, Shyama Prasad Vidyalaya Lodhi Estate, New Delhi 110003

Abstract- The present study aims to determine the interaction of three naturally occurring compounds; eugenol, cis- isoeugenol and methyl eugenol with the binding site of SARS-CoV19 virus. Eugenol is a natural compound which is found extensively in tulsi (Basil) and clove. To understand the geometries and their chemical behavior, density functional theory (DFT) energy calculations and Natural Bond Orbital (NBO) analysis of all three compounds were performed. Global reactivity descriptors were calculated to examine reactivity of the molecules. To understand the drug-likeness of these compounds, Adsorption, Distribution, Metabolism and Excretion (ADME) descriptors were calculated. This was followed by molecular docking studies with SARS-CoV19 spike protein. The efficacy of these compounds as potential drugs for Covid-19 infection was tested by comparing the results with some already known potent drugs. These drugs were Fingolimod, Favipiravir, Chloroquine and Remdesivir. The results show that the molecules, in particular, Eugenol can act as potential inhibitors of SARS-CoV19 virus. This prediction could be further validated by subsequent experimental and clinical studies.

Keywords: Binding Affinity, Docking, ADME, SARS-Cov19, DFT

INTRODUCTION

Severe acute respiratory syndrome coronavirus 2 (SARS-CoV19), which is popularly known as Covid-19, is a highly pathogenic virus of zoonotic origin. It causes a highly transmissible disease which leads to mild to severe respiratory problems in humans. The first case of Covid-19 was recorded on December 8, 2019 in Wuhan, China. Since then, the number of cases has increased at an alarming rate, influencing millions of people across the world. Many recent studies have proven the efficacy of natural products as

potential inhibitors of SARS-CoV19[1]-[4]. Eugenol or 4-allyl-1-hydroxy-2-methoxybenzene is a naturally occurring molecule, found in angiospermic plants and possess a mild aromatic odor of clove and spicy taste[5]. Eugenol comes under the class of phenylpropanes such as anethol, cinnamaldehyde and estragole[6]. Eugenol is partially soluble in water which is an important property in medicines formulation[7]. It has gained importance in research because of its potential role in diminishing and preventing chronic diseases such as cancer, inflammatory reactions, and other serious health conditions[8]. Besides eugenol, cis-isoeugenol and methyl eugenol also has various applications[6]. Methyl eugenol is used as a tang in many food items, in toiletries, detergents for aroma, in some pesticide formulations and as an insect crowd puller. Eugenol are phenolic monoterpenes[6] (it contains an allyl chain which is substituted at para position with respect to the hydroxyl group)[9]. It is well-known that plants possess medicinal value and from ancient times they are used for medicinal purposes[10]. Although Eugenol is majorly extracted from clove buds, stems and leaves[11] but it is also found in many plants like tulsi, cinnamon, lemon balm and nutmeg[12]. Different concentrations of eugenol can be extracted from different plants[12]. Being antiseptic in nature, it is used as a bactericide in mouthwash[13]. Eugenol behaves as a radioprotective molecule[14]. Before coming in contact to γ – radiation, administrating eugenol orally bring down the levels of micronuclei in the polychromatic erythrocytes[15].

This work aims to test the efficacy of eugenol, cis-isoeugenol and methyl eugenol as potential drugs against SARS-CoV19 through molecular docking

studies[16],[17]. Prior to docking, the three molecules were subjected to DFT calculations to understand their properties and chemical reactivity.

COMPUTATIONAL METHODOLOGY

To understand the chemistry of eugenol, cis-isoeugenol and methyl eugenol, DFT calculations and NBO analysis were performed using Gaussian 09 software[18]. B3LYP/6-311G** basis set[19]-[21], was selected for DFT calculations. IR, UV-Visible and NMR spectra were generated in DMSO solvent. These molecules were then subjected to ADME screening using SwissADME tool [22] and molecular docking using Autodock vina[23]. The analysis of docked poses was done in Biovia Discovery studio [24]. To examine the effectiveness of these molecules as drugs, calculations were also carried out on four known drugs, Fingolimod, Remdesivir, Chloroquine and Fepiviravir. In this way, the possibility of these new

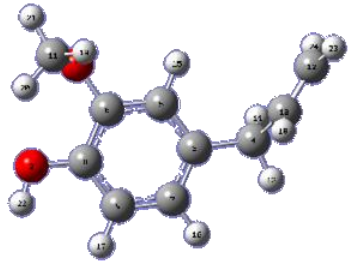
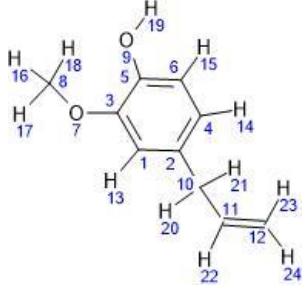
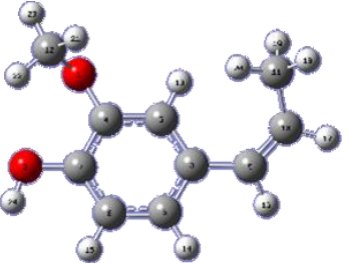

compounds capable of acting as inhibitors against corona virus was tested.

RESULTS AND DISCUSSIONS

DFT Calculations

The three molecules viz. eugenol, cis-isoeugenol and methyl eugenol were geometry optimized in gas phase. The optimized structures along with their numbering scheme are shown in Table 1. This was followed by frequency calculations which revealed absence of imaginary frequency. The IR vibrational frequencies were scaled by a factor of 0.9679 and the zero-point energies by 0.9877 to account for the anharmonicity corrections, and the scaled zero-point energies were added to the calculated energies to give the final energies [25]. A detailed description of the IR frequencies of the three molecules is reported in Table S1 (Supporting Information).

Table 1 Optimized geometries (along with numbering scheme) of Eugenol, cis-Isoeugenol and Methyl eugenol (Color codes: Grey: carbon; white: hydrogen; red: oxygen)

Eugenol		
Cis-Isoeugenol		

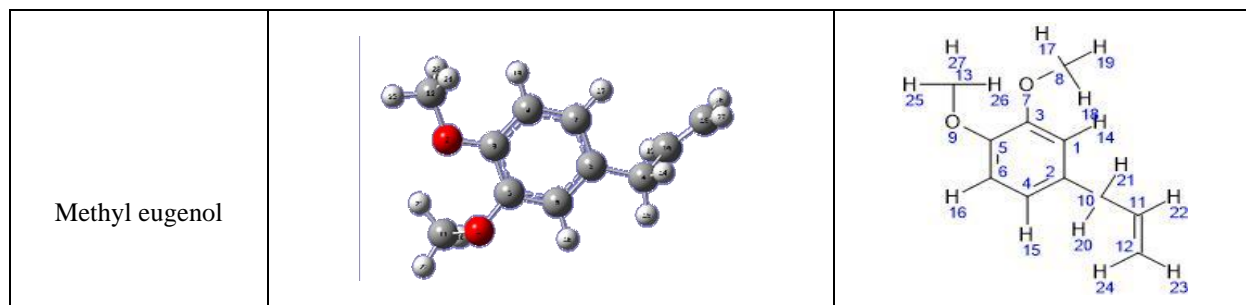


Table 2 Global reactivity descriptors of Eugenol, cis-Isoeugenol and Methyl eugenol

Molecules	HOMO (Ha)	LUMO (Ha)	μ (Ha)	η (Ha)	HLG (Ha)	S (Ha ⁻¹)	Ω (Ha)
Eugenol	0.22537	0.02031	-0.12284	0.10253	0.20506	0.051265	0.073587
Cis-Isoeugenol	0.21500	0.03070	-0.12285	0.09215	0.18430	0.046075	0.081889
Methyl eugenol	0.21932	0.01731	-0.11832	0.101005	0.20201	0.050503	0.069296

On comparing UV-Vis spectra of all the three species, it was found that cis-isoeugenol has maximum value of λ_{max} (Table S2) which is expected because in case of cis-isoeugenol, double bond present outside benzene system also enters in conjugation with benzene. The dipole moment values for all the three species showed that they all are non-polar.

In order to study reactivity of these molecules, several global reactivity descriptors[26],[27] were computed (Table 2). The results reveal that cis-isoeugenol has lowest HOMO-LUMO gap (HLG) among three species which indicates that cis-isoeugenol is most reactive. This is further confirmed by lowest value of chemical potential (η). Global softness (S) value for eugenol and methyl eugenol is almost same which indicates that their electronic cloud can be easily perturbed. Global electrophilicity index (Ω) has highest value for cis-isoeugenol indicating its high tendency to accept electron density.

Total energy and Thermodynamic parameters

Investigation of total energy and thermodynamic parameters (Table 3) of the three molecules indicates that methyl eugenol is most stable. The total energy, enthalpy and free energies are comparable for eugenol and cis-isoeugenol, which reflects their similar stability.

Table 3 Total energy and thermodynamic parameters of Eugenol, cis-Isoeugenol and Methyl eugenol

Molecules	Total Energy (Ha)	Enthalpy (kcal/mol)	Free energy (kcal/mol)
Eugenol	-538.8473	-538.64	-538.69
cis-Isoeugenol	-538.8527	-538.64	-538.69
Methyl eugenol	-578.1560	-577.92	-577.97

NBO Analysis

NBO analysis [28]-[33] was performed for a detailed understanding of the charge transfer within the system (Table S3-S5). The interpretation for analysis of the three molecules is given below.

Eugenol

First seven $\pi \rightarrow \pi^*$ and two $\pi^* \rightarrow \pi^*$ transitions suggest delocalisation of π electron density on the aromatic ring. Lone pair of O2 interacts with π^* molecular orbital of C8-C9 bond which suggests the involvement of this lone pair in resonance with benzene ring. Lone pair of O1 interacts with π^* molecular orbital of C5-C6 bond and σ^* molecular orbital of C11-H19 bond due to resonance effect and hyper conjugative effect

respectively. Electron density from O1 is transferred to σ^* molecular orbital of C6-C8 bond and C5-C6 bond due to hyper conjugative effect.

cis-Isoeugenol

First seven $\pi \rightarrow \pi^*$ and three $\pi^* \rightarrow \pi^*$ transitions suggest delocalisation of π electron density of the aromatic ring and C9-C10 bond. Lone pair of O1 and O2 interacts with π^* molecular orbital of C4-C5 bond and C7-C8 bond respectively which suggests the involvement of lone pair of O1 and O2 in resonance with benzene ring. Lone pair of O2 interacts less with π^* molecular orbital of C4-C7 bond (IE=0.52 kcal/mol) which is due to the involvement of lone pair of O1 in resonance with π^* molecular orbital of C4-C7 bond (IE=5.81 kcal/mol). Lone pair of O1 interacts with σ^* molecular orbital of C12-H21 bond due to hyper conjugative effect.

Methyl Eugenol

First six $\pi \rightarrow \pi^*$ and one $\pi^* \rightarrow \pi^*$ transitions suggest delocalisation of π electron density of the aromatic

ring. Lone pair of O2 and O1 interacts with π^* molecular orbital of C8-C9 bond and C5-C6 bond due to resonance effect. Lone pair of O2 transfers electron density to σ^* molecular orbital of C12-H23 bond and C12-H24 bond due to hyperconjugative effect. Similarly lone pair of O1 interacts with σ^* molecular orbital of C12-H23 bond C11-H21 bond with an interaction energy of 5.77 kcal/mol.

Drug-likeness of molecules

To understand the drug-likeness of the compounds, ADME (Adsorption, Distribution, Metabolism and excretion) screening for the compounds was performed (Table S6) using SwissADME[22]. The physicochemical properties, pharmacokinetics and drug-likeness of these molecules were obtained. Moreover, properties of four compounds that are already in use for the treatment of covid infection, Fingolimod, Favipiravir, Chloroquine and Remdesivir were also calculated. This was done to draw a comparison between the known drugs and proposed drugs.

Table 4 Drug-likeness properties of molecules under investigation

Compound	#H-bond acceptors	#H-bond donors	Lipinski #violation	Ghose #violations	Veber #violations	Egan #violation	Muegge #violation	Bioavailability Score	Lead-likeness #violation
Eugenol	2	1	0	0	0	0	1	0.55	1
Methyl Eugenol	2	0	0	0	0	0	1	0.55	1
cis-Isoeugenol	3	3	0	0	1	0	0	0.55	2
Fingolimod	4	2	0	4	0	0	1	0.55	1
Favipiravir	3	1	0	0	0	0	0	0.55	1
Chloroquine	2	1	0	0	0	0	0	0.55	2
Remdesivir	12	4	2	3	2	1	3	0.17	2

To check the drug-likeness of any molecule, Lipinski's rule of five should be considered[34]. It can be seen from Table 4 and Table S6 (Supporting Information) that all ligands follow Lipinski's rule of five except Remdesivir. Remdesivir has molecular weight greater than 500 Da and hydrogen bond acceptors greater than 10 hence, it violates Lipinski's rule of five. This also results into drug being firmly bound to the body cells. This may be one of the reasons that leads to major side effects by Remdesivir. Hence, it is important for a drug to be moderately bound so that it is safely eliminated from the body in the end. Rest of the six molecules have H-bond donors and acceptors under 5, which falls under acceptable range.

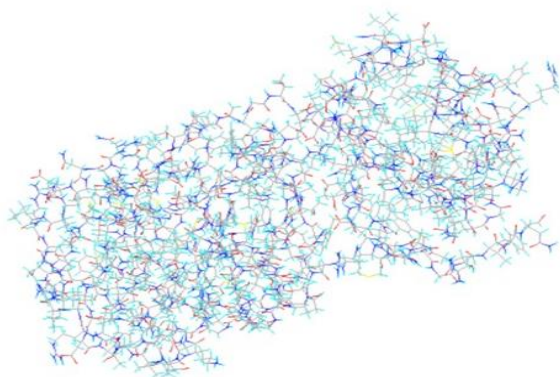
Non zero values for Ghose, Veber and Egan parameters lead to violations from drug-likeness as explained by Diana and co-authors[22]. Bioavailability score is equal for all other molecules except for Remdesivir. Maximum lead-likeness violations (2) are observed in the case of cis-Isoeugenol, Chloroquine and Remdesivir. The results indicate that eugenol and methyl eugenol show promising results and can be considered as potent drugs to treat covid infections. The remaining parameters calculated by SwissADME are provided in Table S6.

Molecular Docking

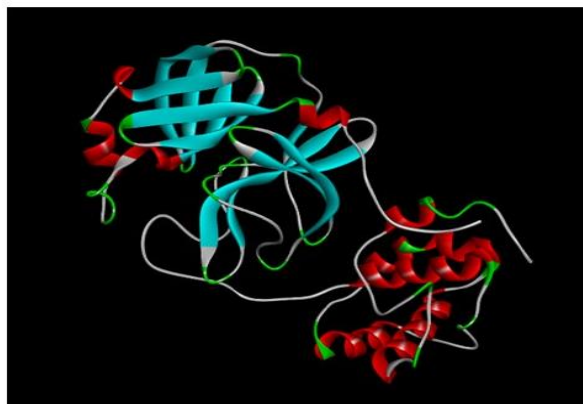
Protein Preparation

The structure of SARS CoV-19 virus with *PDB ID- 6LU7* was selected from RCSB (Research Collaboratory for Structural Bioinformatics) protein data bank[35]. Protein preparation was done using open source BIOVIA Discovery Studio[24]. The aim

of protein preparation is to separate the native ligand from the binding site so that these sites can be used for docking process. The prepared protein is shown in Figure 1(a) and 1(b) in ball and stick model and ribbon form respectively.



(a)



(b)

Figure 1 Structure of the prepared protein (Pdb ID: 6LU7) (a) In ball and stick form (b) In ribbon form

Ligand Library Preparation

A library of 7 ligands comprising of eugenol, methyl eugenol, cis-Isoeugenol, fingolimod, favipiravir, chloroquine and remdesivir was prepared.

Molecular Docking

The molecular docking approach was used to study interaction between ligands and SARS Cov-19 protein. In this paper, blind docking of the protein was done using the grid box coordinate settings. This ensures that the best interaction takes place between the ligands and the binding sites. Autodock vina software[23] was used for the molecular docking study.

Docking Scores

The results obtained from the molecular docking is shown in the Table 5.

Table 5 Binding affinity of all seven ligands

Name of the Ligand	Binding Affinity(Kcal/mol)
Eugenol	-5.5
Methyl Eugenol	-4.7
Fingolimod	-5.3
Favipiravir	-5.3
cis-Isoeugenol	-5.5
Chloroquine	-5.3
Remdesivir	-6.6

The binding affinity represents how firmly a ligand can bind to the spike protein of the virus. As a result of this binding, the binding sites gets occupied and are not free to bind the body cells. Table 5 shows binding affinity of eugenol is better than fingolimod, favipiravir and chloroquine. Although the binding affinity of remdesivir is more than eugenol but the side effects caused by remdesivir cannot be neglected[36]. On the other hand, eugenol being a natural product shows no or less side effects. The rmsd (root mean square deviation) values are generally used for ligands which show different conformations at binding sites of a protein. According to the geometrical and physical nature of the cavity, the values of highest binding affinities for different conformations were generated and the deviation between these values are compared. The highest binding affinity is compared to itself hence the value for rmsd/ub (upper band) and rmsd/lb(lower band) is zero. The order of their binding affinity is mentioned below.

Remdesivir >Eugenol = cis-Isoeugenol > Fingolimod = Favipiravir = Chloroquine > Methyl eugenol

The ligands having high negative binding affinity signify stable interactions between ligand and protein. After a comparison analysis, it can be said

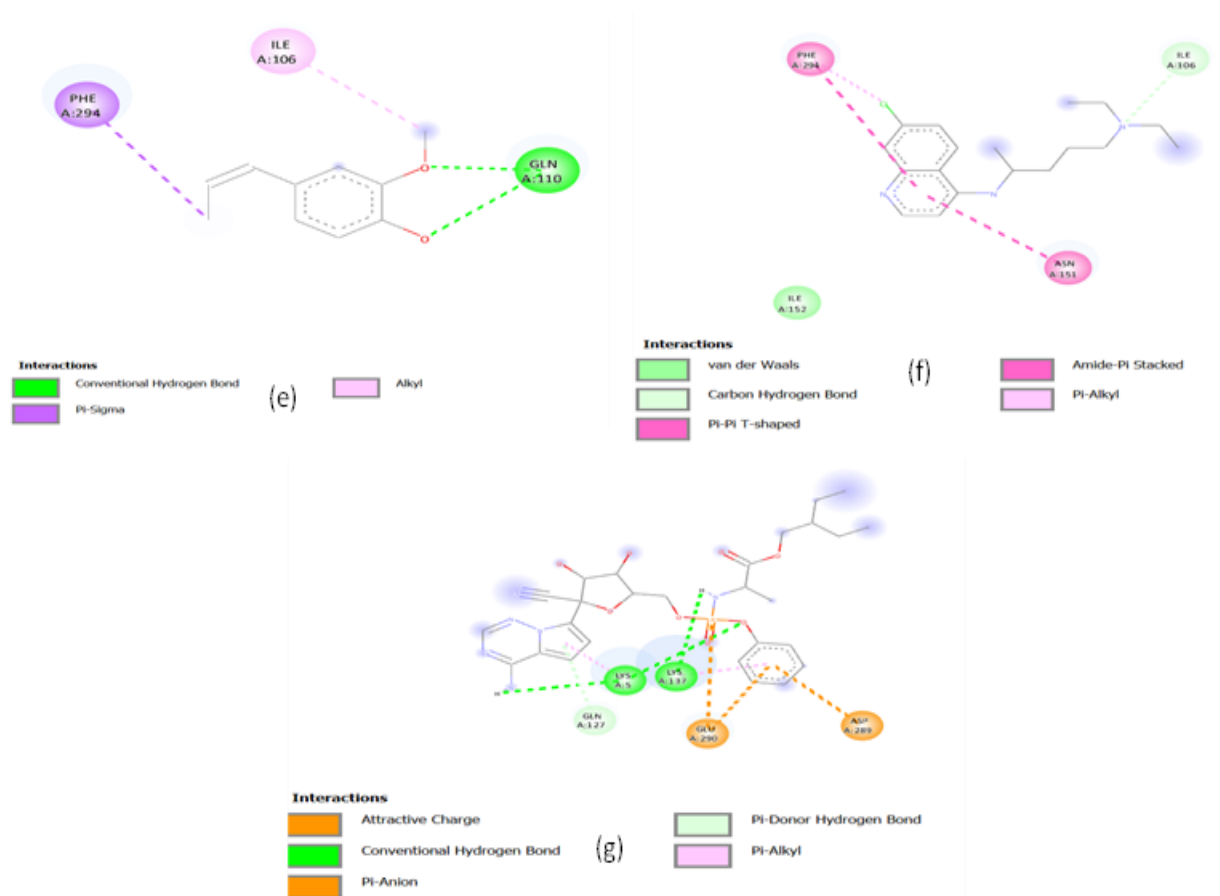


Figure 2 The 2D interaction diagram of the ligands with protein 6LU7 binding sites: (a) Eugenol (b) Methyl Eugenol (c) Fingolimod and (d) Favipiravir (e) cis-Isoeugenol, (f) Chloroquine (g) Remdesivir

Isoeugenol, Chloroquine and Remdesivir, the amino acids which are responsible for the binding of drug to protein are PHE A:294, ILE A:106, GLN A:110; PHE A:294, ILE A:106, ASN A:151 and GLN A:127, LYS A:5, LYS A:137, GLN A:290, ASP A:289 respectively. This shows there are some common binding units which interact with the drug candidates to cause its inhibition. The hydroxyl group in eugenol and methyl eugenol makes it more convenient to interact with the target protein and bind the sites which are responsible for binding with the body cells. This causes inhibition of viral protein, which in turn prevents spread of infection in body.

CONCLUSION

The present study deals with the molecular docking study of three ligands, eugenol, methyl eugenol and cis-Isoeugenol for inhibition of spike protein of SARS-CoV19 virus. The molecular properties such as

global reactivity descriptors, thermodynamic parameters, spectra, NBO analysis were calculated to understand reactivity and of the molecules. Further, drug-likeness, and binding affinity towards protein were calculated using SwissADME. To understand the effectiveness of these ligands as potent drugs, a comparison study was carried out with already known drugs, fingolimod, favipiravir, chloroquine and remdesivir. The results show that cis-Isoeugenol perform poorly in ADME analysis and hence have less drug-likeness. Methyl eugenol has least binding affinity amongst all the docked ligands. However, eugenol passed the ADME analysis and also showed the second highest binding affinity (after Remdesivir) amongst all the docked ligands. From our study, it can be proposed that eugenol is very effective against the inhibition of SARS-CoV19 virus. Additionally, being a natural product, it is safe to consume with minimal or no side effects.

ACKNOWLEDGEMENT

Authors are thankful to ARSD College and Prof. Amit Kumar, Dyal Singh College for supporting this work.

REFERENCE

- [1] Narkhede, R. R., Pise, A. V., Cheke, R. S., Shinde, S. D. (2020). Recognition of natural products as potential inhibitors of COVID-19 main protease (Mpro): In-silico evidences. *Natural products and Bioprospecting*, 10 (5), 297-306.
- [2] Ben-Shabat, S., Yarmolinsky, L., Porat, D., Dahan, A. (2020). Antiviral effect of phytochemicals from medicinal plants: applications and drug delivery strategies. *Drug Delivery and Translational Research*, 10 (2), 354-367.
- [3] Srivastava, A. K., Kumar, A., Misra, N. (2020). On the Inhibition of COVID-19 Protease by Indian Herbal Plants: An In Silico Investigation. arXiv preprint arXiv:2004.03411.
- [4] Marwal, A., Meena, M., Gaur, R.K.(2021) Molecular docking studies of coronavirus Proteins with Medicinal Plant-Based Phytochemicals, *Defence Life Science Journal*, 6(1), pp. 56-62.
- [5] Koeduka, T. et al., (2006) Eugenol and isoeugenol, characteristic aromatic constituents of spices, are biosynthesized via reduction of a coniferyl alcohol ester: *Proceedings of the National Academy of Sciences of the United States of America*, 103(26), pp.10128-10133.
- [6] Bendre, R., Rajput, J., Bagul, S. & Karandikar, P.(2016) *Nat Prod Chem & Res*, 4 (1), pp. 4893-4906.
- [7] Schäfer, E. & Zandbiglari, T.(2003) *Int endod j*, 36 (10), pp. 660-669.
- [8] Fujisawa, S. & Murakami, Y. (2016), *Adv exp med biol*, 929 pp.45-66.
- [9] "Record name: Eugenol," *CHEBI*. <http://www.ebi.ac.uk/chebi/searchId.do?chebiId=CHEBI:4917> (accessed Jan 11, 2022).
- [10] Dubey, R. & Pandey, S. K., *Synthesis of Medicinal Agents from Plants, Chapter 7 - Medicinally important constituents of tulsi (Ocimum spp.)* (Eds. Elsevier), 2018, 151.
- [11] Kamatou, G. P., Vermaak, I. & Viljoen, A. M. (2012), *Molecules (Basel, Switzerland)*, 17 (6) pp.6953-81.
- [12] Raja, M. R. C., Srinivasan, V. S., Selvaraj, S. & Mahapatra, S. K.(2015), *Pharm Anal Acta*, 6 (367), pp.1-6.
- [13] Dorman, H. J. D. & Deans, S. G. (2000), *J Appl Microbiol*, 88 (2), pp. 308-16.
- [14] Alcaraz, M., Armero, D., Martinez-Beneyto, Y., Castillo, J., Benavente-Garcia, O., Fernandez, H., Alcaraz-Saura, M. & Canteras, M. (2011), *Dentomaxillofac Radiol*, 40(5), pp. 310-4.
- [15] Tiku, A. B., Abraham, S. K. & Kale, R. K. (2004), *J Radiat Res*, 49(5), pp. 335-42.
- [16] Kakkar, R., Azad, N. & Gahlot, P. (2012), *Int. Rev. Biophys. Chem. (IREBIC)*, 3, pp. 163-167.
- [17] Azad, N., Bhandari, M. & Kakkar, R. (2016), *J. Biochem. Mol. Biol. Res.* 2, pp.139-151.
- [18] Frisch, M. J. et al., *Gaussian 09, Revision C.01* (G. Inc., Wallingford, 2010).
- [19] Becke, A. D. (1988a) *J. Chem. Phys.* 88, pp. 2547-2553.
- [20] Becke, A. D. (1988b) *Phys. Rev. A*. 38, pp. 3098-3100.
- [21] Vosko, S. H., Wilk, L. & Nusair, M. (1980) *Can. J. Phys.* 58, pp. 1200-1211.
- [22] Daina A, Michielin O & Zoete V, *Sci Rep*, 7 (2017) 42717.
- [23] Trott, O. & Olson, A. J. (2010), *Journal of Computational Chemistry*, 31, pp. 455-461.
- [24] BIOVIA D S (2016) Discovery Studio Modeling Environment, Release 2017, San Diego Dassault Systèmes available at <https://www.3dsbiovia.com/products/collaborative-science/biovia-discovery-studio>
- [25] Andersson, M. P. & Uvdal, P. (2005) *J. Phys. Chem. A*. 109, pp. 2937-2941.
- [26] Marten, B., Kim, K., Cortis, C., Friesner, R. A., Murphy, R. B., Ringnalda, M. N., Sitkoff, D. & Honig, B. (1996) *J. Phys. Chem.* 100, pp. 11775-11788.
- [27] Tannor, D. J., Marten, B., Murphy, R., Friesner, R. A., Sitkoff, D., Nicholls, A., Ringnalda, M., Goddard, W. A. & Honig, B. (1994) *J. Am. Chem. Soc.* 116, pp. 11875-11882.
- [28] Wolinski, K., Hinton, J. F. & Pulay, P. (1990) *J. Am. Chem. Soc.* 112, pp. 8251-8260.
- [29] Bauernschmitt, R. & Ahlrichs, R. (1996), *Chem. Phys. Lett*, 256, pp. 454-464.

- Casida, M.E., Jamorski, C., Casida, K.C., & Salahub, D.R. (1998). *Journal of Chemical Physics*, 108, pp. 4439-4449.
- [30] Stratmann, R. E., Scuseria, G. E., & Frisch, M. J. (1998). *Journal of Chemical Physics*, 109, pp. 8218-8224.
- [31] Padmanabhan, J., Parthasarathi, R., Subramanian, V., Chattaraj, P. (2007), *J. Phys. Chem. A*, 111, pp. 1358-1361.
- [32] Lipinski, C. A., *Drug Discovery Today: Technologies*, 1(4), pp. 337-341.
- [33] Berman, H. M., Westbrook, J., Feng, Z., Gilliland, G., Bhat, T. N., Weissig, H., Shindyalov, I. N. & Bourne, P. E. (2000), *Nucleic Acids Res.* 28(1), pp.235-42.
- [34] Pardo, J., Shukla, A. M., Chamarthi, G. & Gupte, A. (2020), *Drugs Context.* 22(9), pp. 4-14.

Supporting Information

Table S1 IR frequencies of Eugenol, cis-isoeugenol and methyl eugenol

Molecule	Frequency (Intensity)	Description
Eugenol	1303.66(249.1592)	Antisymm stretch C6-C8-O2 coupled with bending mode of C9-H17 and C4-H14
	1540.18(153.7444)	Symm stretch of C6-C8-C9 coupled with bending mode of C9-H17, C7-H16 and C5-H15
	3012.80(88.2458)	Symm stretch of Methyl group coupled with symm stretch of H13-C4-H14
	1187.99(88.1411)	Bending mode of O2-H22, C9-H17, C7-H16H15 and C5-H15
	3836.40(71.8911)	Stretching mode of O2-H22
	308.86(70.1230)	Bending O2-H22
	1044.97(64.4914)	Stretching mode of C11-O1 coupled with bending mode of C9-H17 and C5-H15
	1358.12(64.0228)	Antisymm stretching mode of C6-C8-C9 and C5-C3-C7 coupled with bending mode of H22-O2-C8, C7-H16, C5-H15 and C4-H13.
Cis-Isoeugenol	1317.84(228.2442)	Antisymm stretch of O1-C4-C7 coupled with bending mode of C8-H15, C9-H16, C10-H17, C5-H13 and O2-H24
	1537.04(146.1397)	Antisymm stretch of O1-C4-C7 coupled with symm stretch of C4-C7-C8 and bending mode of C8-H15, C5-H13, C6-H14.
	1128.84(83.1607)	Stretching mode of O1-C4 coupled with bending mode of O2-H24 and C6-H14
	3835.25(82.5868)	Stretching mode of O2-H24r
	1287.75(81.5364)	C3-C6-C8 symm stretch coupled with stretch of O1-C4-C5(antisymm) and O2-C7 and bending mode of C5-H13, C9-H16 and C10-H17
	1187.89(69.3645)	Bending mode of O2-H24, C8-H15, C6-H14 and C5-H13
	3011.71(67.4576)	Symm stretch of methyl group
	307.44(66.7404)	Bending mode of O2-H24
	1044.39(61.3041)	Stretching mode of O1-C12 coupled with bending mode of C5-H13 and C8-H15
1259.77(54.2102)	Stretching of O1-C4 coupled with bending of C12-O1, C12-H21, C12-H22, C7-C4-C5, O2-H24, C6-H14 and C10-H17	
Methyl Eugenol	1292.73(224.5650)	Stretching of C9-C7, O1-C6-C8 (antisymm), C6-C8-O2 (antisymm) coupled with bending of C9-H18, C4-H14, C11-H20, C11-H21, C12-H23 and C12-H24
	1537.37(190.9787)	Symm stretch of C6-C8-C9 and C5-C3-C7 coupled with bending mode of C9-H18, C7-H17, C5-H16, C12-H23, C12-H24 and C12-H25
	1248.16(101.3157)	Stretching of C8-O2 and O1-C6 coupled with bending of C5-H16, C7-H17, C9-H18, C12-H23, C12-H24, C12O2, C11-H20, C11-H21 and C4-H15
	1148.24(97.2224)	Stretching of O2-C12 coupled with bending of C5-H16, C7-H17, C9-H18

	1045.38(80.5794)	Stretching of O1-C11 coupled with bending of C7-C3-C5, C5-H16 and C9-H18
	3010.55(74.5736)	Symm stretch of methyl group corresponding to C11
	3004.34(63.1622)	Symm stretch of methyl group corresponding to C12
	1056.41(56.4860)	O2-C12 stretch coupled with bending of C5-C6-C8
	1310.04(52.7177)	Two bending modes corresponding to H14-C4-H15 and C10-H19 are coupled
	1504.29(45.2787)	Bending of methyl group corresponding to C12

Table S2 UV-Visible spectroscopic parameters of Eugenol, cis-isoeugenol and methyl eugenol

Molecule	Dipole moment (Debye)	*EE1 (nm)	EE2 (nm)	EE3 (nm)
Eugenol	2.1933	254.71 (**0.0496)	236.8 (0.1066)	233.91 (0.0303)
cis-Isoeugenol	2.0268	273.93 (0.1746)	260.43 (0.4168)	246.97 (0.0046)
Methyl eugenol	2.1022	256.79 (0.0816)	239.58 (0.148)	234.59 (0.0186)

*Excitation Energy

**Figures in parenthesis are oscillator strength

Table S3 Natural Bond Orbital (NBO) analysis of eugenol

Donor Orbital	Acceptor Orbital	Interaction Energy in kcal/mol (IE)
π (C3-C7)	π^* (C5-C6)	20.19
π (C3-C7)	π^* (C8-C9)	19.72
π (C5-C6)	π^* (C3-C7)	19.28
π (C5-C6)	π^* (C8-C9)	20.82
π (C8-C9)	π^* (C3-C7)	19.27
π (C8-C9)	π^* (C5-C6)	17.37
n2(O2)	π^* (C8-C9)	25.86
π^* (C8-C9)	π^* (C3-C7)	165.62
π^* (C8-C9)	π^* (C5-C6)	287.71
n2(O1)	π^* (C5-C6)	9.67
n2(O1)	σ^* (C11-H19)	5.8
n1(O2)	σ^* (C8-C9)	5.74
n1(O1)	σ^* (C6-C8)	5.87
σ (C12-H24)	σ^* (C10-H18)	5.33
σ (C12-H23)	σ^* (C4-C10)	6.21
σ (C10-H18)	σ^* (12-H24)	4.92
σ (C4-H13)	σ^* (C3-C5)	4.51
σ (C5-H15)	σ^* (C3-C7)	4.39
σ (C5-H15)	σ^* (C6-C8)	4.04
σ (C7-C9)	σ^* (O2-C8)	4.37
σ (C7-H16)	σ^* (C3-C5)	4.48
σ (C8-C9)	σ^* (C6-C8)	4
n2(O1)	σ^* (C5-C6)	4.35

Table S4 Natural Bond Orbital (NBO) analysis of cis-Isoeugenol

Donor Orbital	Acceptor Orbital	Interaction Energy in kcal/mol (IE)
π (C3-C7)	π^* (C4-C5)	21.08
π (C3-C7)	π^* (C7-C8)	20.52
π (C3-C6)	π^* (C9-C10)	11.42

π (C4-C5)	π^* (C3-C6)	18.27
π (C4-C5)	π^* (C7-C8)	20.82
π (C7-C8)	π^* (C3-C6)	20.04
π (C9-C10)	π^* (C3-C6)	8.84
π^* (C7-C8)	π^* (C3-C6)	188.08
π^* (C7-C8)	π^* (C4-C5)	286.98
π^* (C3-C6)	π^* (C9-C10)	38.32
n2(O1)	σ^* (C4-C5)	4.31
n1(O2)	σ^* (C7-C8)	5.76
n2(O2)	σ^* (C7-C8)	25.94
n1(O2)	σ^* (C4-C7)	0.52
n2(O1)	π^* (C4-C5)	9.52
σ (C5-H13)	σ^* (C3-C6)	4.11
σ (C5-H13)	σ^* (C4-C7)	4.14
σ (C6-H8)	σ^* (O2-C7)	4.33
σ (C6-H14)	σ^* (C3-C5)	4.25
σ (C9-H16)	σ^* (C3-C7)	4.02
σ (C9-H16)	σ^* (C10-C11)	7
σ (C10-H17)	σ^* (C3-C9)	7.22
σ (C11-H19)	σ^* (C9-C10)	5.12

Table S5 Natural Bond Orbital (NBO) analysis of Methyl eugenol

Donor Orbital	Acceptor Orbital	Interaction Energy in kcal/mol (IE)
π (C3-C7)	π^* (C5-C6)	20.57
π (C3-C7)	π^* (C8-C9)	19.71
π (C5-C6)	π^* (C3-C7)	19.32
π (C5-C6)	π^* (C8-C9)	19.99
π (C8-C9)	π^* (C3-C7)	19.49
π (C8-C9)	π^* (C5-C6)	17.92
π^* (C8-C9)	π^* (C3-C7)	172.08
n2(O2)	π^* (C8-C9)	28.15
n2(O1)	π^* (C5-C6)	9.14
n2(O1)	σ^* (C11-H20)	5.77
n2(O2)	σ^* (C12-H23)	5.67
n2(O2)	σ^* (C12-H24)	5.56
n1(O1)	σ^* (C6-C8)	5.96
n2(O1)	σ^* (C5-C6)	4.49
σ (C5-H16)	σ^* (C3-C7)	4.39
σ (C5-H16)	σ^* (C6-C8)	4.3
σ (C7-C9)	σ^* (O2-C8)	4.52
σ (C7-H17)	σ^* (C3-C5)	4.45

σ (C10-H19)	σ^* (C13-H27)	4.94
σ (C13-H26)	σ^* (C4-C10)	6.19
σ (C13-H27)	σ^* (C10-H19)	5.31
σ (C11-H19)	σ^* (C9-C10)	5.12

Table S6 SwissADME analysis of various molecules under investigation

Property	Eugenol	Methyl Eugenol	Fingolimod	Favipiravir	Cis-Iso Eugenol	Chloroquine	Remdesivir
Molecule	Molecule 1	Molecule 2	Molecule 3	Molecule 4	Molecule 5	Molecule 6	Molecule 7
MW (Da)	164.2	178.23	164.2	307.47	157.1	319.87	602.58
#Heavy atoms	12	13	12	22	11	22	42
#Aromatic heavy atoms	6	6	6	6	6	10	15
Fraction C _{sp3}	0.2	0.27	0.2	0.68	0	0.5	0.48
#Rotatable bonds	3	4	2	12	1	8	14
#H-bond acceptors	2	2	2	3	4	2	12
#H-bond donors	1	0	1	3	2	1	4
MR	49.06	53.53	49.86	94.32	32.91	97.41	150.43
TPSA	29.46	18.46	29.46	66.48	88.84	28.16	213.36
iLOGP	2.37	2.65	2.47	3.76	0.39	3.95	3.52
XLOGP3	2.27	2.52	3.04	4.16	-0.56	4.63	1.91
WLOGP	2.13	2.43	2.33	3.2	-0.57	4.62	2.21
MLOGP	2.01	2.3	2.01	3.01	-1.3	3.2	0.18
Silicos-IT Log P	2.48	3	2.31	4.62	0.69	4.32	-0.05
Consensus Log P	2.25	2.58	2.43	3.75	-0.27	4.15	1.56
ESOL Log S	-2.46	-2.61	-3.01	-3.78	-0.8	-4.55	-4.12
ESOL Solubility (mg/mL)	5.69E-01	4.37E-01	1.60E-01	5.14E-02	2.50E+01	9.05E-03	4.58E-02
ESOL Solubility (mol/L)	3.47E-03	2.45E-03	9.74E-04	1.67E-04	1.59E-01	2.83E-05	7.59E-05
ESOL Class	Soluble	Soluble	Soluble	Soluble	Very soluble	Moderately soluble	Moderately soluble
Ali Log S	-2.53	-2.55	-3.32	-5.26	-0.84	-4.95	-6.01
Ali Solubility (mg/mL)	4.90E-01	4.98E-01	7.78E-02	1.67E-03	2.29E+01	3.61E-03	5.84E-04
Ali Solubility (mol/L)	2.98E-03	2.79E-03	4.74E-04	5.44E-06	1.46E-01	1.13E-05	9.69E-07
Ali Class	Soluble	Soluble	Soluble	Moderately soluble	Very soluble	Moderately soluble	Poorly soluble
Silicos-IT LogSw	-2.79	-3.5	-2.42	-5.76	-1.42	-6.92	-4.77
Silicos-IT Solubility (mg/mL)	2.65E-01	5.62E-02	6.27E-01	5.32E-04	6.04E+00	3.86E-05	1.03E-02
Silicos-IT Solubility (mol/L)	1.61E-03	3.16E-04	3.82E-03	1.73E-06	3.85E-02	1.21E-07	1.71E-05
Silicos-IT class	Soluble	Soluble	Soluble	Moderately soluble	Soluble	Poorly soluble	Moderately soluble
GI absorption	High	High	High	High	High	High	Low
BBB permeant	Yes	Yes	Yes	Yes	No	Yes	No
Pgp substrate	No	No	No	Yes	No	No	Yes
CYP1A2 inhibitor	Yes	Yes	Yes	No	No	Yes	No
CYP2C19 inhibitor	No	No	No	No	No	No	No
CYP2C9 inhibitor	No	No	No	No	No	No	No
CYP2D6 inhibitor	No	No	No	Yes	No	Yes	No
CYP3A4 inhibitor	No	No	No	Yes	No	Yes	Yes
log Kp (cm/s)	-5.69	-5.6	-5.14	-5.22	-7.66	-4.96	-8.62
Lipinski #violations	0	0	0	0	0	0	2

Ghose #violations	0	0	0	0	4	0	3
Veber #violations	0	0	0	1	0	0	2
Egan #violations	0	0	0	0	0	0	1
Muegge #violations	1	1	1	0	1	0	3
Bioavailability Score	0.55	0.55	0.55	0.55	0.55	0.55	0.17
PAINS #alerts	0	0	0	0	0	0	0
Brenk #alerts	1	1	0	0	0	0	1
Lead-likeness #violations	1	1	1	2	1	2	2
Synthetic Accessibility	1.58	1.71	1.81	2.27	2.08	2.76	6.33